Optimizing the Grafting Density of Tethered Chains to Alter the Local Glass Transition Temperature of Polystyrene near Silica Substrates: The Advantage of Mushrooms over Brushes

Xinru Huang and Connie B. Roth\*

Department of Physics, Emory University, Atlanta, Georgia 30322, USA

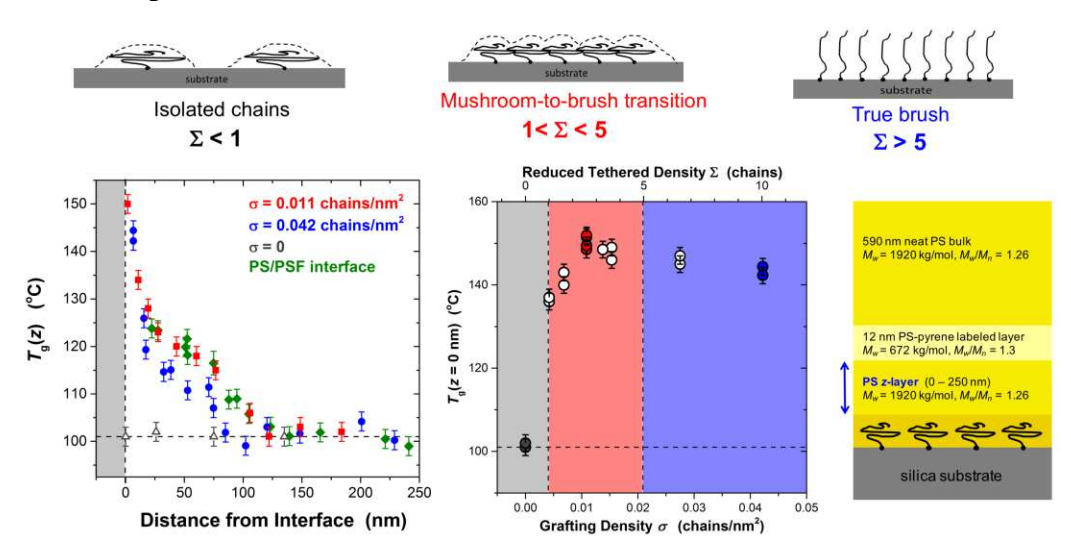
\* To whom correspondence should be addressed. cbroth@emory.edu

Submitted to ACS Macro Letters, January 8, 2018;

Accepted February 7, 2018; Published February 9, 2018

**ABSTRACT:** We measured the local glass transition temperature  $T_g(z)$  of polystyrene (PS) as a function of distance z from a silica substrate with end-grafted chains using fluorescence, where competing effects from the free surface have been avoided to focus only on the influence of the tethered-interface. The local  $T_g(z)$  increase next to the chain-grafted substrate is found to exhibit a maximum increase of  $49 \pm 2$  K relative to bulk at an optimum grafting density that corresponds to the mushroom-to-brush transition regime. This perturbation to the local  $T_g(z)$  dynamics of the matrix is observed to persist out to a distance  $z \approx 100$ -125 nm for this optimum grafting density before bulk  $T_g$  is recovered, a distance comparable to that previously observed by Baglay and Roth [*J. Chem. Phys.* **2017**, *146*, 203307] for PS next to the higher- $T_g$  polymer polysulfone.

## **TOC Graphic:**



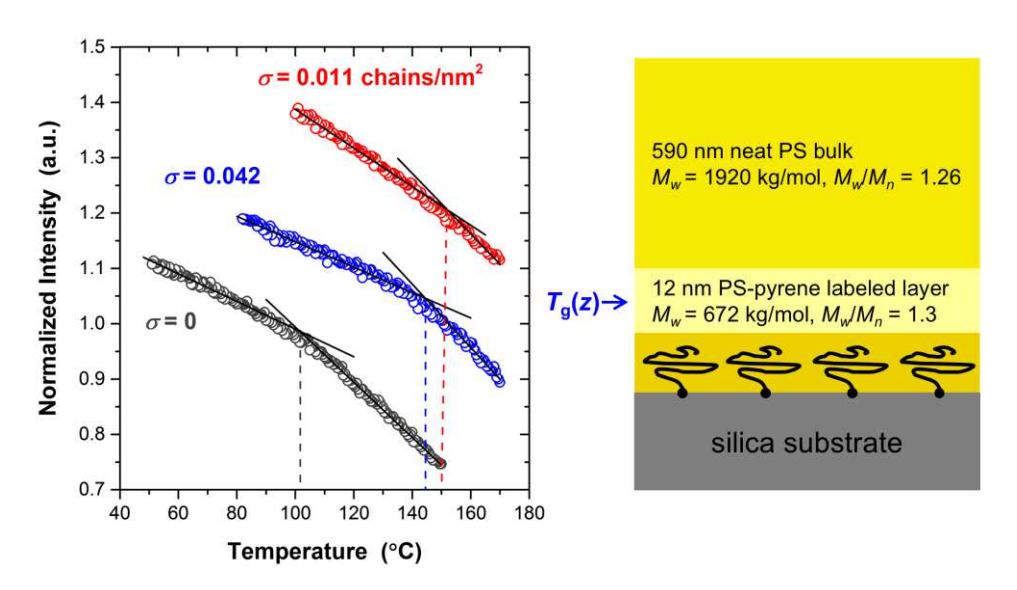
Direct interrogation of how end-tethered chains affect the local properties of a neighboring polymer matrix has been little studied, but widely utilized to alter adhesion, lubrication, and improve matrix reinforcement in polymer nanocomposites. 1-7 There are few local experimental techniques that can interrogate material properties next to such buried interfaces, usually leaving local properties to be inferred from global macroscopic measurements or investigated by theoretical and simulation methods.<sup>2,8,9</sup> The influence tethered chains can have on the neighboring matrix is complicated by various interconnected parameters such as grafting density, surface coverage, tethered-chain length, matrix interpenetration, and substrate curvature, with the macroscopic properties of nanocomposites being further affected by the filler content and dispersion.<sup>6,7</sup> Studies on thin films provide an accessible planar geometry where the grafting density can be well controlled, serving as a simplified system to mimic polymer nanocomposites. 10-12 However, most thin film studies investigating substrates with grafted chains are additionally affected by the competing effects of the free surface. 13-21 Here, we purposely avoid such competing effects of the free surface and experimentally map the local glass transition temperature  $T_g(z)$  as a function of distance from a tethered-chain interface using a localized fluorescence method.

Studies of the average glass transition temperature  $T_g(h)$  of thin polystyrene (PS) films with substrate grafted chains date back to Keddie and Jones in 1995. Over the years studies have reported both increases  $^{14,15,18}$  and decreases  $^{16}$  in the average  $T_g(h)$  value relative to films of equivalent thickness h with no grafted chains. Generally, these changes are only observed for very thin films  $h \lesssim 30$  nm, and can be sufficiently small to appear as effectively no change. Recently, Hénot et al. have made great efforts to compare and correlate different studies based on the grafting density and ratio of matrix-to-grafted chain lengths, ultimately concluding that the grafted chains have little to no effect on the measured average film  $T_g(h)$ . However, such measurements are complicated by the presence of a strong, and potentially dominating, free surface effect. Lan and Torkelson used fluorescence to measure the local  $T_g$  of grafted chains within a thin film finding large variations in local  $T_g$  within the films with increases as high as  $\sim$ 35 K near the substrate, while the near free surface region was reduced by  $\sim$ 15 K. This large variation in local  $T_g$  within the film suggests there is strong competition between free surface and chain-tethered substrate effects such that much benefit would be gained from isolating only the impact of the chain-tethered substrates.

In the present work, we have created a sample geometry that allows us to measure the local glass transition temperature  $T_g(z)$  as a function of distance from an end-grafted PS substrate. End-grafted polystyrene substrates were created by spin-coating a film of monocarboxy-terminated polystyrene (PS-COOH) ( $M_w = 101.8 \text{ kg/mol}$ ,  $M_w/M_n = 1.03$ ) onto either silicon wafers or silica substrates cleaned by washing in ~10 vol% hydrochloric acid for 20 s. These films were annealed under vacuum at 170 °C for 1.5 h to establish covalent bonding between PS-COOH and Si-OH, and then washed in a 90 °C toluene bath for 20 min to remove any ungrafted chains and subsequently rinsed in acetone and DI water, dried with nitrogen gas and annealed overnight in a vacuum oven at room temperature; a procedure following previous works. <sup>13-15</sup> The final dry-bush thickness  $h_{\text{brush}}$  was measured by ellipsometry (Woollam M-2000) for those samples made on silicon wafers modeling the PS layer with a standard Cauchy model  $n(\lambda) = A + B/\lambda^2 + C/\lambda^4$ , fitting A and B with C held at the bulk value, and including a 1.25 nm native oxide layer for the silicon substrate. <sup>22</sup> The grafting density  $\sigma$  was calculated as  $\sigma = \frac{\rho N_A \text{ hbrush}}{M_n}$ , <sup>23</sup> where  $\rho = 1.045 \text{ g/cm}^3$  was taken to be the bulk density of PS, <sup>24</sup>  $N_A$  is Avogadro's number, and  $M_n$  is the PS-COOH number average molecular weight.

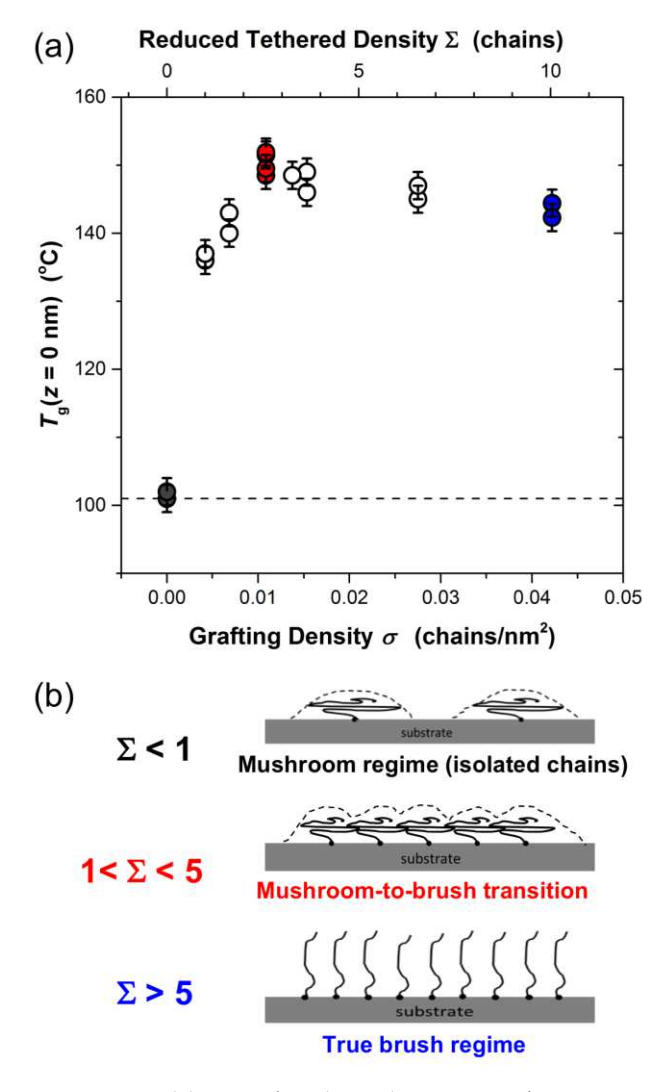
Multilayer samples as depicted in Figures 1 and 3 were then assembled by floating on additional PS layers of known thickness made from either neat PS ( $M_w = 1920 \text{ kg/mol}$ ,  $M_w/M_n = 1920 \text{ kg/mol}$ ,  $M_w/M_n = 1920 \text{ kg/mol}$ ) 1.26) or pyrene-labeled PS ( $M_{\rm w} = 672 \text{ kg/mol}$ ,  $M_{\rm w}/M_{\rm n} = 1.3$ , with 1.4 mol% pyrene<sup>25,26</sup>). The dry-brush layer and first PS layer floated atop were annealed separately at 170 °C for 2 h to ensure good interpenetration of the tethered chains with the neighboring PS matrix.<sup>27,28</sup> Prior to the fluorescence measurements, the entire multilayer stack was annealed at 170 °C for 20 min to consolidate the stack into a single material, but keep the pyrene-labeled layer localized, as well as remove thermal history of the sample before  $T_g(z)$  was measured. In some samples, the PSpyrene layer was also lightly crosslinked using UV light to limit diffusion at such high temperatures (see Supporting Information for further details). Following our previous works, <sup>25,26,29</sup> pyrene fluorescence emission at 379 nm was monitored on cooling at 1 °C/min for 3 s every 27 s while exciting at 330 nm (band passes 5-6 nm). The local  $T_{\rm g}(z)$  was determined by the change in slope of the temperature-dependence of the fluorescence intensity, as established by Torkelson and coworkers, 30-32 a value that has been shown to agree well with the change in thermal expansion coefficient by ellipsometry and differential scanning calorimetry (DSC) in bulk.

Figure 1 compares the local  $T_{\rm g}(z=0)$  next to end-tethered substrates as a function of grafting density  $\sigma$ . The multilayer samples assembled for this place the  $12\pm 1$  nm pyrene-labeled layer directly next to the dry-brush layer, which were then separately annealed together such that the pyrene-labeled chains become well intermixed with the tethered chains. A  $590\pm 5$  nm bulk neat PS layer is then added to avoid competing effects from the free surface. Thus, the  $T_{\rm g}(z=0)$  value being reported here is for a  $(12~{\rm nm}+h_{\rm brush})$  layer next to the silica substrate. When no chains are grafted to the substrate, the 12-nm pyrene-labeled layer reports a  $T_{\rm g}(z=0)=101\pm 2~{\rm ^oC}$ , equal to the bulk value for PS, and in agreement with that previously measured by Ellison and Torkelson. In contrast, with the addition of end-tethered chains to the substrate, the local  $T_{\rm g}(z=0)$  is increased dramatically: for  $\sigma=0.011$  chains/nm² ( $h_{\rm brush}=1.7\pm 0.2~{\rm nm}$ ),  $T_{\rm g}(z=0)=150\pm 2~{\rm ^oC}$ ;  $\sigma=0.042$  chains/nm² ( $h_{\rm brush}=6.6\pm 0.2~{\rm nm}$ ),  $T_{\rm g}(z=0)=143\pm 2~{\rm ^oC}$ ; where these values represent the average of multiple samples. These increases in local  $T_{\rm g}(z=0)$  appear large given previous reports on end-grafted PS films,  $^{13-16,18,19}$  but in those studies competing free surface effects were also present. In the current study, the addition of the top bulk neat PS layer allows us to isolate only the effect of the end-tethered substrate.



**Figure 1.** Sample geometry used to measure the local  $T_g(z=0)$  next to end-tethered substrates with different grafting densities  $\sigma$ , where the temperature-dependent fluorescence intensity curves show large increases in this local  $T_g$  value.

In Figure 2, we plot this  $T_g(z=0)$  value measured next to end-tethered substrates as a function of grafting density. We observe a maximum  $T_g(z=0)$  increase at  $\sigma = 0.011$  chains/nm<sup>2</sup>  $(h_{\rm brush} = 1.7 \pm 0.2 \text{ nm})$  suggesting an optimum grafting density exists for greatest  $T_{\rm g}$ reinforcement of the PS matrix. This result may seem surprising initially, but makes sense if one considers the limits at low and high grafting density. Clearly at  $\sigma = 0$ , we must recover bulk  $T_g$ of PS, as has been previously demonstrated<sup>30</sup> for this non-interacting substrate. At extremely high grafting densities, the tight chain packing of the tethered chains in the true brush regime will limit interpenetration of the free (untethered) matrix chains, 33,34 resulting in a decrease in the measured  $T_g(z)$  of the neighboring PS matrix as the two become decoupled. For example, the recent study by Lan and Torkelson<sup>17</sup> measured the local  $T_g$  of pyrene-labeled PS brushes made by a "grafting from" technique that results in much higher grafting densities. Their closest measurement to our current study is the local  $T_g$  of an 11-nm thick brush with  $\sigma = 0.3$  chains/nm<sup>2</sup> covered with a 101-nm thick neat PS overlayer resulting in a local  $T_g \approx 126$  °C for the brush chains next to the silica substrate. This value is consistent with our data presented in Fig. 2a if we were to extrapolate an estimate out to this value of  $\sigma$  that is an order of magnitude larger than our largest  $\sigma$ .



**Figure 2.** (a) Local  $T_g(z=0)$  measured next to end-tethered substrates as a function of grafting density  $\sigma$  (bottom axis) and reduced tethered density  $\Sigma$  (top axis). (b) Cartoon illustrating the three different regimes associated with increasing  $\Sigma$  as the tethered chains go from isolated mushrooms to highly stretched brushes.

A better measure of how much end-tethered chains cover a substrate is the reduced tethered density  $\Sigma = \pi R_g^2 \ \sigma$ ,  $^{23,35,36}$  which multiplies the grafting density  $\sigma$  (chains/nm²) by the projected area of the surface ( $\pi R_g^2$ ) each tethered chain nominally covers, where the radius of gyration  $R_g = 8.7$  nm for our molecular weight. This enables characterization of the grafted surface into different regimes. Values of  $\Sigma < 1$  refer to the "mushroom" regime where the chains are still predominately isolated, while the "true brush" regime where the grafting density is high enough for chains to becomes highly stretched is generally observed for  $\Sigma > 5$ . The

mushroom-to-brush transition regime where the conformations of neighboring chains begin overlapping happens between  $1 < \Sigma < 5$ , the precise onset of which can vary somewhat from system to system. <sup>23,35,36</sup> Interestingly, we observe that the optimum grafting density  $\sigma = 0.011$  chains/nm² that shows the maximum  $T_g(z=0)$  increase occurs at a value of  $\Sigma = 2.6$ , near the middle of the mushroom-to-brush transition (well within the "wet" brush regime  $\sigma \sqrt{N} < 1$ ). <sup>38,39</sup> It is worth noting that nearly all previous studies that have investigated  $T_g$  changes in thin films due to grafted chains are very close to or well within the true brush regime,  $\Sigma \gtrsim 5$ , <sup>13-19</sup> with the general belief being that higher grafting density should lead to larger effects. <sup>19</sup> Our results suggest more is not necessarily better and that a lower grafting density can lead to a higher  $T_g$  increase. However, we caution that blindly applying this reasoning to polymer nanocomposites may cause additional complications, as low grafting densities often lead to increased nanoparticle aggregation. <sup>6</sup>

The extent to which end-tethered chains can interpenetrate into a matrix depends not only on the grafting density, but also on the relative difference in molecular weight between the tethered and matrix chains. For the case of a polymer melt where the brush is chemically identical to the matrix, the scaling behavior of the penetration length L over which the endtethered chains extend from the substrate has been well studied. 33,34 For our case where the matrix chain length P is larger than the tethered chain length N, the tethered chains retain their ideal conformation from the mushroom regime all the way up to the beginning of the true brush regime such that  $L \sim N^{\frac{1}{2}}$ . This means that within the mushroom-to-brush transition regime, as the grafting density increases, the number of matrix chains P that interpenetrate into the brush region L decreases continuously, while the tethered chains retain their ideal conformation. Finally at the start of the true brush regime, little interpenetration will occur when the tethered chains must finally stretch beyond their ideal chain conformations to accommodate further increases in grafting density. We can estimate the amount of chain interpenetration present for our optimum grafting density  $\sigma = 0.011$  chains/nm<sup>2</sup> by comparing the initial dry brush thickness ( $h_{brush} = 1.7 \pm$ 0.2 nm) to the penetration length L. For an ideal chain conformation, we estimate  $L \approx 2R_g \approx 17$ nm, giving a volume fraction  $\phi = \frac{h_{\text{brush}}}{L} \approx 0.1$  for the tethered chains within this layer L near the substrate. This estimate for L is consistent with theoretical calculations by Matsen and Gardiner<sup>38</sup> where an extrapolation down to our grafting density gives a value of  $\approx 18$  nm. In addition, neutron reflectivity profiles by Clarke<sup>27</sup> for deuterated PS-COOH tethered chains ( $M_{\rm w}$  = 79.8 kg/mol) with grafting density  $\sigma \approx 0.074$  chains/nm<sup>2</sup> in a hydrogenated PS matrix ( $M_{\rm w} = 500.8$  kg/mol or 8,000 kg/mol) show the volume fraction depth profile for the grafted chains extending out to  $\approx 18\text{-}20$  nm.

What seems surprising is that the observed maximum increase in  $T_g(z=0)$  occurs when only ~10% of this near substrate region is comprised of tethered chains. Little is known about how tethered chains would cause an increase in  $T_{\rm g}$ . The closest theoretical efforts are those that have tried to account for attractive substrate interactions. For example, Long and Lequeux<sup>40</sup> developed a percolation model of the glass transition that defined  $T_{\rm g}$  based on when dynamically slow regions percolate across the sample, envisioning that attractive substrate interactions increased the fraction of slow regions. Lipson and Milner<sup>41</sup> developed this idea into a more detailed picture of how a profile in local  $T_g(z)$  increase would look near substrates with attractive interactions, a prediction that is qualitatively consistent with our experimental observations shown below. Within such a framework one could imagine how a few extra slow domains that included segments of chains tethered to the substrate could have a large influence on such a percolation rigidity transition. However, chain connectivity is not typically associated with the glass transition. The molecular weight dependence of  $T_g(M_n)$  saturates to  $\approx 100$  °C for PS at  $M_n \approx$ 20 kg/mol, 42,43 which has been correlated with when chain dynamics asymptotically display Gaussian behavior, 44,45 as local chain flexibility near free chain ends are different. This suggests that tethered chain ends may in a similar fashion alter local mobility of the chain influencing local  $T_g$ . Experimentally, recent studies by Foster et al. 46,47 have shown that substrate tethered chains can significantly slow surface relaxation times of PS films, even when films include substantial amounts of untethered matrix chains, which likely results from the increased entropic penalty to stretch tethered chains. 48,49

Figure 3 addresses how far this strong perturbation to local  $T_g$  near the end-tethered substrate propagates into the neighboring polymer matrix. To locally measure  $T_g(z)$  as a function of distance from the substrate, we insert a high molecular weight neat PS spacer layer of thickness z = 0 - 250 nm between the dry brush and 12-nm thick pyrene-labeled PS layer. Again to ensure good interpenetration of the grafted chains with the PS matrix, while still avoiding diffusion of the pyrene-labeled layer, the PS z-layer and dry brush were separately annealed at 170 °C for 2 h prior to floating on the remaining layers. Figure 3 plots the local  $T_g(z)$  measured as a function of distance from the end-tethered substrate for the optimum and maximum grafting

densities shown in Fig. 2. We also include data for  $T_g(z)$  with zero grafting density that confirms no  $T_g$  increase is observed for PS next to bare silica. To accommodate the slight differences in dry brush thickness  $h_{\text{brush}}$  with increasing grafting density, we defined the distance from the interface (x-axis of Fig. 3) as  $z + h_{\text{brush}}$ , although this correction is minor on the scale of Fig. 3. For both grafting densities shown, the  $T_g(z)$  perturbation is observed to propagate far from the interface ( $z \sim 100 \text{ nm}$ ) before bulk  $T_g$  is recovered, a distance much larger than the end-tethered chains extend from the substrate,  $L \approx 2$   $R_g \approx 17$  nm. Interestingly, the  $T_g(z)$  perturbation for the optimum grafting density  $\sigma = 0.011$  chains/nm², which gave the maximum  $T_g(z = 0)$  in Fig. 2, appears to influence the PS matrix out to a somewhat greater distance ( $z \approx 100$ -125 nm) from the interface, compared with that ( $z \approx 75$ -100 nm) for the higher grafting density of  $\sigma = 0.042$  chains/nm².

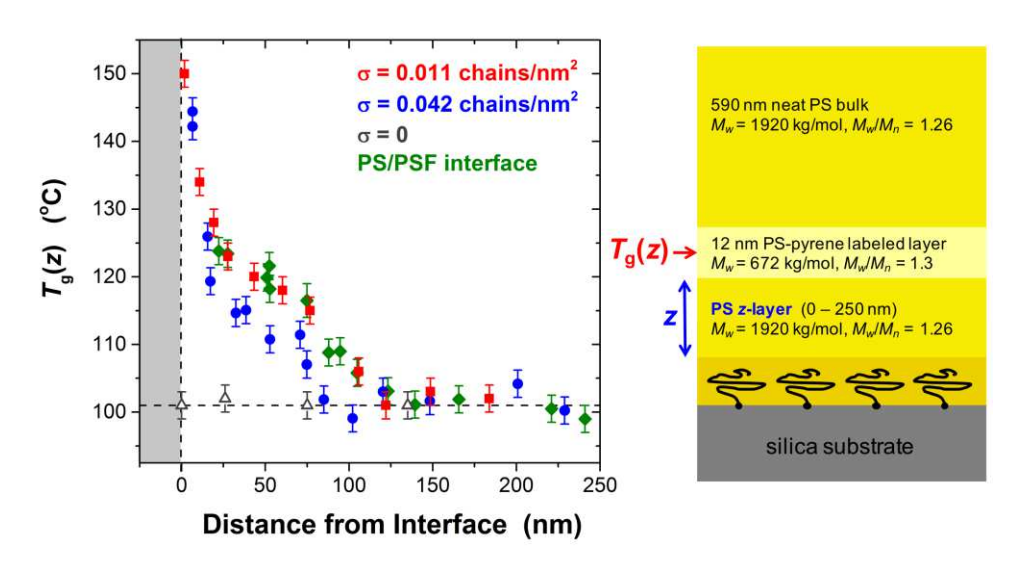


**Figure 3.** Local  $T_g(z)$  profiles extending from end-tethered substrates for grafting densities  $\sigma = 0.011$  chains/nm<sup>2</sup> (red squares) and  $\sigma = 0.042$  chains/nm<sup>2</sup> (blue circles), as well as for substrates with no grafted chains ( $\sigma = 0$ , gray triangles). For comparison, data from Baglay and Roth<sup>26</sup> for the  $T_g(z)$  profile in PS next to polysulfone (PSF,  $T_g^{PSF} = 186$  °C) is shown as green diamonds.

For comparison, Figure 3 also includes data from Baglay and Roth<sup>26</sup> for the  $T_g(z)$  profile measured in PS next to a polymer-polymer interface with polysulfone (PSF). As the bulk  $T_g$  of PSF ( $T_g^{PSF} = 186$  °C) is much higher than that of PS, this polymer-polymer interface is somewhat analogous to that of the end-tethered silica interface studied in the present work. Figure 3 shows

that the  $T_g(z)$  profile in PS next to the PS/PSF interface is comparable to that observed in PS next to the end-tethered silica substrate at the optimum grafting density of  $\sigma = 0.011$  chains/nm<sup>2</sup>. In their paper, Baglay and Roth<sup>26</sup> discussed three possible differences for why dissimilar polymer-polymer interfaces may show such long-ranged  $T_g(z)$  perturbations, in contrast to a polymer-free surface: increased breadth of the interfacial width, chain connectivity across the interface, and increased interfacial roughness. The results of the present study suggest that chain connectivity may play the dominant role in causing such long-ranged  $T_g(z)$  perturbations, with factors such as interfacial breadth<sup>50</sup> and substrate roughness<sup>51,52</sup> having more limited effects.

**Acknowledgments.** The authors gratefully acknowledge support from the National Science Foundation Polymers Program (DMR-1151646 and DMR-1709132) and Emory University. We also thank Roman Baglay, Michael Thees, and Eric Weeks for useful discussions.

**Supporting Information Available**: The Supporting Information is available free of charge on the ACS Publications website at DOI: 10.1021/acsmacrolett.XXXXXXX. Sample preparation details and experimental methods, along with control measurements conducted to verify that lightly crosslinking the pyrene-labeled layer using UV light does not affect the fluorescence measurements.

## **References:**

- (1) Milner, S. T. Polymer Brushes. *Science* **1991**, *251*, 905–914.
- (2) Schadler, L. S.; Kumar, S. K.; Benicewicz, B. C.; Lewis, S. L.; Harton, S. E. Designed Interfaces in Polymer Nanocomposites: a Fundamental Viewpoint. *MRS Bulletin* **2007**, *32*, 335–340.
- (3) Bansal, A.; Yang, H.; Li, C.; Benicewicz, R. C.; Kumar, S. K.; Schadler, L. S. Controlling the Thermomechanical Properties of Polymer Nanocomposites by Tailoring the Polymer-Particle Interface. *J Polym Sci, Part B: Polym Phys* **2006**, *44*, 2944–2950.
- (4) Oh, H.; Green, P. F. Polymer Chain Dynamics and Glass Transition in Athermal Polymer/Nanoparticle Mixtures. *Nature Materials* **2009**, *8*, 139–143.
- (5) Maillard, D.; Kumar, S. K.; Fragneaud, B.; Kysar, J. W.; Rungta, A.; Benicewicz, B. C.; Deng, H.; Brinson, L. C.; Douglas, J. F. Mechanical Properties of Thin Glassy Polymer Films Filled with Spherical Polymer-Grafted Nanoparticles. *Nano Lett* **2012**, *12*, 3909–3914.

- (6) Kumar, S. K.; Jouault, N.; Benicewicz, B.; Neely, T. Nanocomposites with Polymer Grafted Nanoparticles. *Macromolecules* **2013**, *46*, 3199–3214.
- (7) Kumar, S. K.; Ganesan, V.; Riggleman, R. A. Perspective: Outstanding Theoretical Questions in Polymer-Nanoparticle Hybrids. *J Chem Phys* **2017**, *147*, 020901.
- (8) Holt, A. P.; Bocharova, V.; Cheng, S.; Kisliuk, A. M.; White, B. T.; Saito, T.; Uhrig, D.; Mahalik, J. P.; Kumar, R.; Imel, A. E.; *et al.* Controlling Interfacial Dynamics: Covalent Bonding Versus Physical Adsorption in Polymer Nanocomposites. *ACS Nano* **2016**, *10*, 6843–6852.
- (9) Hall, L. M.; Jayaraman, A.; Schweizer, K. S. Molecular Theories of Polymer Nanocomposites. *Curr Opin Solid St M* **2010**, *14*, 38–48.
- (10) Bansal, A.; Yang, H. C.; Li, C. Z.; Cho, K. W.; Benicewicz, B. C.; Kumar, S. K.; Schadler, L. S. Quantitative Equivalence Between Polymer Nanocomposites and Thin Polymer Films. *Nature Materials* **2005**, *4*, 693–698.
- (11) Rittigstein, P.; Priestley, R. D.; Broadbelt, L. J.; Torkelson, J. M. Model Polymer Nanocomposites Provide an Understanding of Confinement Effects in Real Nanocomposites. *Nature Materials* **2007**, *6*, 278–282.
- (12) Kropka, J. M.; Pryamitsyn, V.; Ganesan, V. Relation Between Glass Transition Temperatures in Polymer Nanocomposites and Polymer Thin Films. *Phys Rev Lett* **2008**, *101*, 075702.
- (13) Keddie, J. L.; Jones, R. A. L. Glass Transition Behavior in Ultra-Thin Polystyrene Films. *Israel J Chem* **1995**, *35*, 21–26.
- (14) Tate, R. S.; Fryer, D. S.; Pasqualini, S.; Montague, M. F.; de Pablo, J. J.; Nealey, P. F. Extraordinary Elevation of the Glass Transition Temperature of Thin Polymer Films Grafted to Silicon Oxide Substrates. *J Chem Phys* **2001**, *115*, 9982–9990.
- Clough, A.; Peng, D.; Yang, Z.; Tsui, O. K. C. Glass Transition Temperature of Polymer Films That Slip. *Macromolecules* **2011**, *44*, 1649–1653.
- (16) Lee, H.; Ahn, H.; Naidu, S.; Seong, B. S.; Ryu, D. Y.; Trombly, D. M.; Ganesan, V. Glass Transition Behavior of PS Films on Grafted PS Substrates. *Macromolecules* **2010**, *43*, 9892–9898.
- (17) Lan, T.; Torkelson, J. M. Substantial Spatial Heterogeneity and Tunability of Glass Transition Temperature Observed with Dense Polymer Brushes Prepared by ARGET ATRP. *Polymer* **2015**, *64*, 183–192.
- (18) Zuo, B.; Zhang, S.; Niu, C.; Zhou, H.; Sun, S.; Wang, X. Grafting Density Dominant Glass Transition of Dry Polystyrene Brushes. *Soft Matter* **2017**, *13*, 2426–2436.
- (19) Hénot, M.; Chenneviere, A.; Drockenmuller, E.; Shull, K.; Léger, L.; Restagno, F. Influence of Grafting on the Glass Transition Temperature of PS Thin Films. *Eur Phys J E* **2017**, *40*, 11.
- (20) Tsui, O. K. C.; Russell, T. P.; Hawker, C. J. Effect of Interfacial Interactions on the Glass Transition of Polymer Thin Films. *Macromolecules* **2001**, *34*, 5535–5539.

- (21) Neubauer, N.; Winkler, R.; Tress, M.; Uhlmann, P.; Reiche, M.; Kipnusu, W. K.; Kremer, F. Glassy Dynamics of Poly(2-Vinyl-Pyridine) Brushes with Varying Grafting Density. *Soft Matter* **2015**, *11*, 3062–3066.
- (22) Huang, X.; Roth, C. B. Changes in the Temperature-Dependent Specific Volume of Supported Polystyrene Films with Film Thickness. *J Chem Phys* **2016**, *144*, 234903.
- (23) Brittain, W. J.; Minko, S. A Structural Definition of Polymer Brushes. *J Polym Sci, Part A: Polym Chem* **2007**, *45*, 3505–3512.
- (24) Orwoll, R. A. Densities, Coefficients of Thermal Expansion, and Compressibilities of Amorphous Polymers. In *Physical Properties of Polymers Handbook*; Mark, J. E., Ed.; Springer: New York, 2007; pp. 93–101.
- (25) Baglay, R. R.; Roth, C. B. Communication: Experimentally Determined Profile of Local Glass Transition Temperature Across a Glassy-Rubbery Polymer Interface with a Tg Difference of 80 K. *J Chem Phys* **2015**, *143*, 111101.
- (26) Baglay, R. R.; Roth, C. B. Local Glass Transition Temperature  $T_g(z)$  of Polystyrene Next to Different Polymers: Hard vs. Soft Confinement. *J Chem Phys* **2017**, *146*, 203307.
- (27) Clarke, C. J. The Kinetics of Polymer Brush Penetration in to a High Molecular Weight Matrix. *Polymer* **1996**, *37*, 4747–4752.
- (28) O'Connor, K. P.; McLeish, T. C. B. "Molecular Velcro": Dynamics of a Constrained Chain Into an Elastomer Network. *Macromolecules* **1993**, *26*, 7322–7325.
- (29) Rauscher, P. M.; Pye, J. E.; Baglay, R. R.; Roth, C. B. Effect of Adjacent Rubbery Layers on the Physical Aging of Glassy Polymers. *Macromolecules* **2013**, *46*, 9806–9817.
- (30) Ellison, C. J.; Torkelson, J. M. The Distribution of Glass-Transition Temperatures in Nanoscopically Confined Glass Formers. *Nature Materials* **2003**, *2*, 695–700.
- (31) Ellison, C. J.; Mundra, M. K.; Torkelson, J. M. Impacts of Polystyrene Molecular Weight and Modification to the Repeat Unit Structure on the Glass Transition-Nanoconfinement Effect and the Cooperativity Length Scale. *Macromolecules* **2005**, *38*, 1767–1778.
- (32) Kim, S.; Hewlett, S. A.; Roth, C. B.; Torkelson, J. M. Confinement Effects on Glass Transition Temperature, Transition Breadth, and Expansivity: Comparison of Ellipsometry and Fluorescence Measurements on Polystyrene Films. *Eur Phys J E* **2009**, *30*, 83–92.
- (33) Aubouy, M.; Fredrickson, G. H.; Pincus, P.; Raphaeel, E. End-Tethered Chains in Polymeric Matrixes. *Macromolecules* **1995**, *28*, 2979–2981.
- (34) Jones, R. A. L.; Richards, R. W. *Polymers at Surfaces and Interfaces*; Cambridge University Press, 1999.
- (35) Kent, M. S. A Quantitative Study of Tethered Chains in Various Solution Conditions Using Langmuir Diblock Copolymer Monolayers. *Macromol Rapid Comm* **2000**, *21*, 243–270.

- (36) Cheng, S. Z. D. *Phase Transitions in Polymers: the Role of Metastable States*; Elsevier Science: Oxford, UK, 2008.
- (37) Fetters, L. J.; Hadjichristidis, N.; Lindner, J. S.; Mays, J. W. Molecular Weight Dependence of Hydrodynamic and Thermodynamic Properties for Well-Defined Linear Polymers in Solution. *Journal of Physical and Chemical Reference Data* **1994**, *23*, 619–640.
- (38) Matsen, M. W.; Gardiner, J. M. Autophobic Dewetting of Homopolymer on a Brush and Entropic Attraction Between Opposing Brushes in a Homopolymer Matrix. *J Chem Phys* **2001**, *115*, 2794–2804.
- (39) Note,  $\Sigma$  is an experimental parameter whose definition is based on the theoretical scaling that mushrooms begin to overlap when the average distance between grafting sites  $\sigma^{-1/2} \approx R_g.^{1,33,34}$  This is in contrast to other definitions of normalized grafting density<sup>15</sup> more commonly used in the theoretical literature that scale  $\sigma$  about the transition point from a "wet" screened (unstretched) brush to a "dry" (stretched) "true" brush at  $\sigma \approx N^{-1/2}.^{33,34}$  According to self-consistent field theory calculations by Matsen and Gardiner, <sup>38</sup> our largest grafting density  $\sigma = 0.042$  chains/nm² should still be within the "wet" brush regime with  $\frac{\sigma N^{1/2}}{a \rho_0} \leq 0.32$ .
- (40) Long, D.; Lequeux, F. Heterogeneous Dynamics at the Glass Transition in Van Der Waals Liquids, in the Bulk and in Thin Films. *Eur Phys J E* **2001**, *4*, 371–387.
- (41) Lipson, J. E. G.; Milner, S. T. Percolation Model of Interfacial Effects in Polymeric Glasses. *Eur Phys J B* **2009**, *72*, 133–137.
- (42) Santangelo, P. G.; Roland, C. M. Molecular Weight Dependence of Fragility in Polystyrene. *Macromolecules* **1998**, *31*, 4581–4585.
- (43) Fox, T. G.; Flory, P. J. The Glass Temperature and Related Properties of Polystyrene: Influence of Molecular Weight. *J Polym Sci* **1954**, *14*, 315–319.
- (44) Ding, Y.; Kisliuk, A.; Sokolov, A. P. When Does a Molecule Become a Polymer? *Macromolecules* **2004**, *37*, 161–166.
- (45) Mirigian, S.; Schweizer, K. S. Dynamical Theory of Segmental Relaxation and Emergent Elasticity in Supercooled Polymer Melts. *Macromolecules* **2015**, *48*, 1901–1913.
- Uğur, G.; Akgun, B.; Jiang, Z.; Narayanan, S.; Satija, S.; Foster, M. D. Effect of Tethering on the Surface Dynamics of a Thin Polymer Melt Layer. *Soft Matter* **2016**, *12*, 5372–5377.
- (47) Akgun, B.; Uğur, G.; Jiang, Z.; Narayanan, S.; Song, S.; Lee, H.; Brittain, W. J.; Kim, H.; Sinha, S. K.; Foster, M. D. Surface Dynamics of "Dry" Homopolymer Brushes. *Macromolecules* **2009**, *42*, 737–741.
- (48) Fredrickson, G. H.; Ajdari, A.; Leibler, L.; Carton, J. P. Surface Modes and Deformation Energy of a Molten Polymer Brush. *Macromolecules* **1992**, *25*, 2882–2889.

- (49) Xi, H.-W.; Milner, S. T. Surface Waves on Polymer Brushes. *Macromolecules* **1996**, *29*, 4772–4776.
- (50) Mirigian, S.; Schweizer, K. S. Influence of Chemistry, Interfacial Width, and Non-Isothermal Conditions on Spatially Heterogeneous Activated Relaxation and Elasticity in Glass-Forming Free Standing Films. *J Chem Phys* **2017**, *146*, 203301.
- (51) Hanakata, P. Z.; Douglas, J. F.; Starr, F. W. Interfacial Mobility Scale Determines the Scale of Collective Motion and Relaxation Rate in Polymer Films. *Nat Commun* **2014**, *5*, 4163.
- (52) Hanakata, P. Z.; Pazmiño Betancourt, B. A.; Douglas, J. F.; Starr, F. W. A Unifying Framework to Quantify the Effects of Substrate Interactions, Stiffness, and Roughness on the Dynamics of Thin Supported Polymer Films. *J Chem Phys* **2015**, *142*, 234907.